

https://doi.org/10.1070/QEL17629

Thermo-optic parameters of potassium titanyl phosphate crystals

S.G. Grechin, P.Ya. Druzhinin, D.G. Kochiev

Abstract. **This paper presents results of a comparative analysis of thermo-optic parameters of potassium titanyl phosphate (KTP) crystals. We demonstrate that some relations for temperature derivatives of their principal refractive indices have limited applicability. We propose that, to more accurately determine these parameters, temperature-noncritical phase matching should be taken into account.**

Keywords: *nonlinear crystals, potassium titanyl phosphate, KTP, thermo-optic parameters, frequency conversion, temperature phase-matching bandwidth.*

Potassium titanyl phosphate, $KTiOPO_4$ (KTP), biaxial crystals [1] have found wide application for nonlinear-optical frequency conversion: generation of harmonics, sum and difference frequency generation, and parametric generation. This is due to their large effective nonlinearity coefficients (d_{eff}) and phase matching bandwidth in combination with a satisfactory optical damage threshold [2]. Their low coercive fields allow one to produce crystals with a regular domain structure in which sss (eee) phase matching ensures record large effective nonlinearity coefficients and angle-noncritical phase matching (ANCPM) [3].

If the phase matching condition is fulfilled, the potentialities of nonlinear crystals for frequency conversion are determined by their effective nonlinearity coefficient and angular, frequency, and temperature phase-matching bandwidths. Analysis of phase matching properties of a crystal requires data on the dispersion of its principal refractive indices $n_i(\lambda)$, where $i = x$, y, or z. To obtain dispersion relations, use is typically made of single- or double-resonance equations (see below), which are often supplemented by Taylor series terms in order to reach the best agreement with experimental data. The most accurate expressions can be obtained using experimentally measured refractive indices $n_i(\lambda)$ and phase matching angles (φ, θ) for various frequency conversion processes. The phase matching angles of KTP crystals are usually measured for the second type of interaction (sff and fsf), which has the largest effective nonlinearity coefficient. All the main results presented below are for this type of phase matching.

The first equations proposed for describing $n_i(\lambda)$ data for KTP crystals included Sellmeier single-resonance equations [4], which were based on a limited set of experimentally measured refractive indices and phase matching angles:

$$n_x^2 = 3.0065 + \frac{0.03901}{\lambda^2 - 0.04251} - 0.01327\lambda^2, \tag{1a}$$

$$n_y^2 = 3.0333 + \frac{0.04154}{\lambda^2 - 0.04547} - 0.01408\lambda^2, \tag{1b}$$

$$n_z^2 = 3.3134 + \frac{0.05694}{\lambda^2 - 0.05658} - 0.01682\lambda^2. \tag{1c}$$

Here and in what follows, λ is expressed in microns. The phase matching angles calculated with the use of these relations for the generation of harmonics and parametric generation (see the table in Ref. [4]) in the wavelength range 1.0–2.4 μm agree rather well with experimental data. Later, more complete experimental data made it possible to obtain the following double-resonance dispersion relations for the $n_i(\lambda)$ of KTP crystals [5]:

$$n_x^2 = 3.29100 + \frac{0.04140}{\lambda^2 - 0.03978} + \frac{9.35522}{\lambda^2 - 31.45571}, \tag{2a}$$

$$n_y^2 = 3.45018 + \frac{0.04341}{\lambda^2 - 0.04597} + \frac{16.98825}{\lambda^2 - 39.43799}, \tag{2b}$$

$$n_z^2 = 4.59423 + \frac{0.06206}{\lambda^2 - 0.04763} + \frac{110.80672}{\lambda^2 - 86.12171}. \tag{2c}$$

There are also other kinds of Sellmeier equations for KTP, referenced by Nikogosyan [2].

Relations (2) ensured agreement between large amounts of calculation results and experimental data for various frequency conversion processes in the wavelength range 0.43--3.54 μm (see the table in Ref. [5]). This determined their practical importance. The $n_i(\lambda)$ calculation results obtained using (1) and (2) are presented in Fig. 1. Relations (2) allow one to find not only phase matching directions for various frequency conversion processes but also angle- and frequency-noncritical phase matching directions and tuning characteristics of parametric oscillators.

To assess the effect of temperature on phase matching properties of crystals, one uses expressions describing $dn_i(\lambda)/dT$ data. As a rule, they supplement known Sellmeier equations. In most cases, such expressions are determined by a Taylor expansion in terms of λ^{-m}, where $m = 0, 1, 2, 3, \ldots$. In 1992,

S.G. Grechin, D.G. Kochiev Prokhorov General Physics Institute, Russian Academy of Sciences, ul. Vavilova 38, 119991 Moscow, Russia; e-mail: GrechinSG@kapella.gpi.ru;
P.Ya. Druzhinin St. Petersburg National Research University of Information Technologies, Mechanics and Optics, Kronverkskii prosp. 49, 197101 St. Petersburg, Russia

Received 4 August 2021
Kvantovaya Elektronika **51** (10) 953–957 (2021)
Translated by O.M. Tsarev

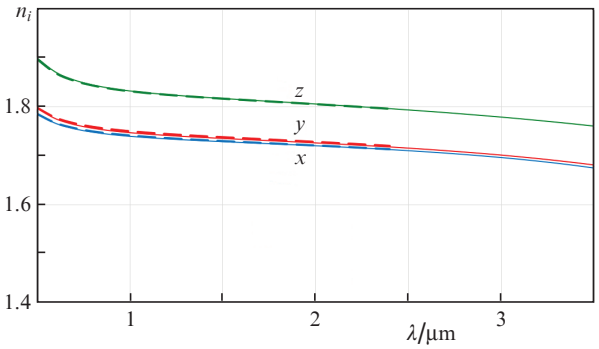

Figure 1. Dispersion curves $n_i(\lambda)$ calculated for KTP crystals using relations (2) (solid lines) and (1) (dashed lines).

taking into account available experimental data and the equations for $n_i(\lambda)$ in Ref. [4], Kato [6] proposed the following relations for $dn_i(\lambda)/dT$ (in °C^{-1}) in the wavelength range 0.53–1.32 μm:

$$\frac{dn_x}{dT} = (0.1323\lambda^{-3} - 0.4385\lambda^{-2} + 1.2307\lambda^{-1} + 0.7709) \times 10^{-5}, \quad (3a)$$

$$\frac{dn_y}{dT} = (0.5014\lambda^{-3} - 2.0030\lambda^{-2} + 3.3016\lambda^{-1} + 0.7498) \times 10^{-5}, \quad (3b)$$

$$\frac{dn_z}{dT} = (0.3896\lambda^{-3} - 1.3332\lambda^{-2} + 2.2762\lambda^{-1} + 2.1151) \times 10^{-5}. \quad (3c)$$

Relations (3) were derived from experimentally determined temperature derivatives of the principal refractive indices and the temperature phase-matching bandwidth for various frequency conversion processes. Kato [6] compared calculation results obtained using (3) and experimental data. Table 1 presents some calculated and experimentally determined values of the phase matching temperature T_{pm}, the φ and θ angles determining phase matching directions, and the temperature phase-matching bandwidth $2\Delta T$. (Here and in what follows, the phase matching bandwidth is represented by $2\Delta T$ because the positive and negative half bandwidths ΔT differ.)

Accuracy of relations (3) can also be ensured by determining the temperatures at which phase matching is directed along one of the principal axes of the crystal. These results are of practical importance because ANCPM along the principal axes of crystals has a large angular bandwidth. In the case of second harmonic generation (SHG) at a wavelength of 1.0795 μm (Nd:YAP) in a KTP crystal, phase matching is possible along the x axis ($\varphi = 0$ and $\theta = 90°$). In this direction, KTP has the largest effective nonlinearity coefficient. As pointed out by Kato [6], no agreement with measurement results reported by Garmash et al. [7] was reached. However, it was found out [8] that they presented results for a KTP crystal grown at various solvent and dopant concentrations, so it could be regarded as a mixed crystal. Garmash et al. [7] thought it unnecessary to specify this in their report. Ou et al. [14] and Abrosimov et al. [15] obtained phase matching along the x axis in the case of SHG at a wavelength of 1.0795 μm (Nd:YAP) in KTP by heating the crystal to temperatures that agreed with calculated ones (Table 1).

In 2002, Kato and Takaoka [5] reported the following dispersion relations $dn_i(\lambda)/dT$ (in °C^{-1}) obtained using more complete experimental data:

$$\frac{dn_x}{dT} = (0.1717\lambda^{-3} - 0.5353\lambda^{-2} + 0.8416\lambda^{-1} + 0.1627) \times 10^{-5}, \quad (4a)$$

$$\frac{dn_y}{dT} = (0.1997\lambda^{-3} - 0.4063\lambda^{-2} + 0.5154\lambda^{-1} + 0.5425) \times 10^{-5} \quad (4b)$$

$$(0.43\ \mu m \leqslant \lambda \leqslant 1.58\ \mu m),$$

Table 1. Calculated and experimentally determined phase matching parameters of a KTP crystal in the case of SHG with sff phase matching.

λ_j/μm		T_{pm}/°C		φ/deg /θ/deg		$2\Delta T$/°C		Ref.
$\lambda_1 = \lambda_2$	λ_3	calculation	experiment	calculation	experiment	calculation	experiment	
0.9942	0.4971	20	20	90/90	90/90	177	175	[9]
1.00246	0.50123	20		71.4/90		TNCPM*		
1.0642	0.5321		20		23.2/90	24.3	24	[10]
			20			97.5	100	[11]
			20		23/90		23.3	[12]
			20	67.7/70.9	67/71	TNCPM*	>210	[12]
			20	45.7/44.0**	45.7/44.0	TNCPM*	>150	[6]
1.0795	0.53975		20	0/87.4	0/85.7			[7]
		63.8	153		0/90	19.9	20	[7]
			20	0/86.88	0/86.7			[13]
			63		0/90		30	[14]
			20	0/87.26	0/87.5	17.5		[15]
		66.9	54	0/90	0/90	22.4		[15]
1.0804	0.5402		20		0/90			[16]
3.0905	1.5453		20	0/66.5	0/66.5			[6]
			20	0/76.5	0/76.5			[6]
3.1842	1.5921		20	90/72.1	90/72.2			[6]
			20	9.9/90	9.5/90			[6]
3.18	1.59		20	0/90		TNCPM*		

* For $n_i(\lambda)$ from Ref. [4] and $dn_i(\lambda)/dT$ from Ref. [6] , there is TNCPM with a temperature phase-matching bandwidth $2\Delta T > 100$ °C for a 1.0-cm-long crystal (calculations were performed using only first-order $dn_i(\lambda)/dT$). ** For ssf phase matching.

$$\frac{dn_z}{dT} = (0.9221\lambda^{-3} - 2.9220\lambda^{-2} + 3.6677\lambda^{-1} - 0.1897) \times 10^{-5} \quad (4c)$$

$$(0.53\ \mu m \leqslant \lambda \leqslant 1.57\ \mu m),$$

$$\frac{dn_z}{dT} = (-0.5523\lambda^{-1} + 3.3920 - 1.7101\lambda + 0.3424\lambda^2) \times 10^{-5} \quad (4d)$$

$$(1.32\ \mu m \leqslant \lambda \leqslant 3.53\ \mu m).$$

The curves in Fig. 2 represent relations (4c) and (4d). Each curve was constructed throughout the transparency region of KTP. The rectangles represent the corresponding applicability limits. The thin lines represent the portions of relations (4) that lie beyond the applicability limits of (4c) and (4d). The two curves 'join' at a wavelength of 1.3 μm. The thick line corresponds to a complete solution over the entire transparency region of KTP, from 0.5 to 4.5 μm.

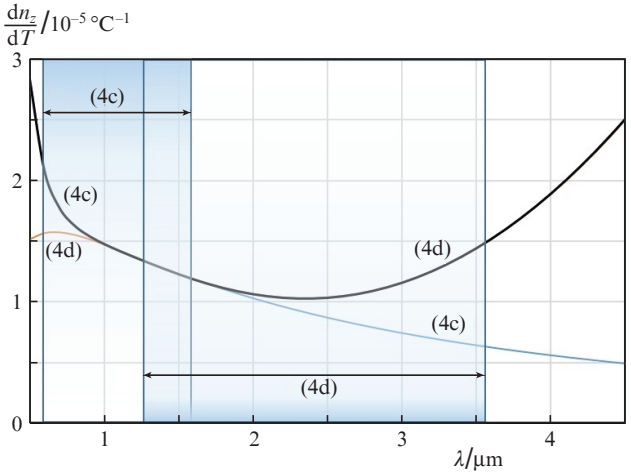

Figure 2. Dispersion curves $dn_z(\lambda)/dT$ calculated for KTP crystals using relations (4c) and (4d). The rectangles represent the applicability limits of these relations.

Figure 3 shows the $dn_i(\lambda)/dT$ curves for all the principal refractive indices from Refs [5, 6] [relations (4) and (3), respectively]. It is well seen that there are a qualitative distinction between the $dn_z(\lambda)/dT$ curves and quantitative distinctions between the $dn_x(\lambda)/dT$ curves, as well as between the $dn_y(\lambda)/dT$ curves. Since (4) is obtained with allowance for experimentally determined temperature phase-matching bandwidths, there is good agreement between calculation results and experimental data for some frequency conversion processes [5] in the principal planes of the crystals. However, as in the case of (3), there is no agreement between calculation results obtained with formulas (4) and the experimental measurement results reported by Garmash et al. [7]. Unfortunately, this is not the only problem.

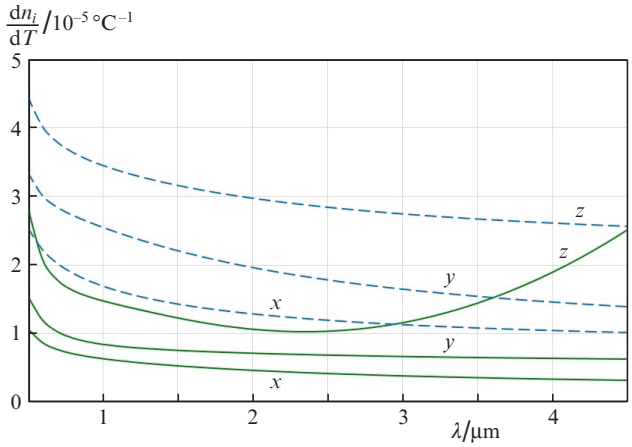

Figure 3. Dispersion curves $dn_z(\lambda)/dT$ calculated for KTP crystals using relations (4) (solid lines) and (3) (dashed lines).

Using relations (1) and (3), we precisely determined the crystal section in which temperature-noncritical phase matching (TNCPM) occurred for sff interaction in SHG of light with a wavelength of 1.0642 μm, which allowed us to obtain $2\Delta T$ above 210 °C [12]. For the same SHG process using (1) and (3) Kato [6] found a section for ssf TNCPM and obtained a temperature bandwidth above 150 °C. If relations (4) are used, TNCPM at a wavelength of 1.0642 μm is impossible for any type of phase matching.

Figure 4 presents calculation results for phase matching angles at which TNCPM is possible in the case of SHG at various fundamental wavelengths. Table 2 lists phase match-

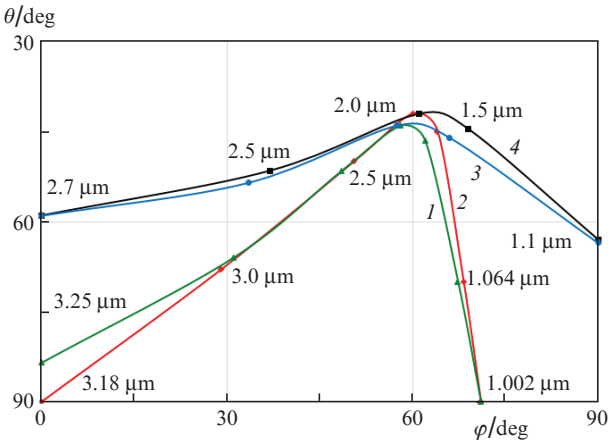

Figure 4. Phase matching directions (φ, θ) for SHG at various wavelengths and various combinations of data for $n_i(\lambda)$ and $dn_i(\lambda)/dT$: curve *1* corresponds to relations (1) and (3); curve *2*, to relations (2) and (3); curve *3*, to relations (1) and (4); and curve *4*, to relations (2) and (4).

Table 2. Phase matching angles calculated for SHG with TNCPM (Fig. 4) using $n_i(\lambda)$ data from Refs [4] (columns 1 and 3) and [5] (columns 2 and 4) and $dn_i(\lambda)/dT$ data from Refs [6] (columns 1 and 2) and [5] (columns 3 and 4) (the numbers of the columns correspond to the numbers of the curves in Fig. 4).

λ/μm	φ/deg/θ/deg			
1.003	–	71/90	–	–
1.022	71/90	70/78	–	–
1.064	68/70	68/70	–	–
1.1	66.5/65.5	66.5/65.5	90/63.5	90/63
1.5	62/46.5	64/45	66/46	69/44.5
2.0	58/44	60/42	57.5/44	61/42
2.5	48.5/51.5	50.5/50	33.5/53.5	37/51.5
2.66	44.5/55	45.5/54	0/59	15/57.5
2.7	43/56	44/55	–	0/59
3.0	31/66	29/68	–	–
3.18	17/76	0/90	–	–
3.25	0/83.5	–	–	–

ing angles for some fundamental wavelengths. In the case of the $dn_i(\lambda)/dT$ data from Ref. [6], TNCPM is possible in the wavelength range from 1.003–1.022 to 3.18–3.25 μm. If data from Ref. [5] are used, this range is considerably narrower.

Figure 5 shows FOM(λ_1,λ_2) distributions [where FOM = $d_{\text{eff}}^2/(n_1n_2n_3)$], analogous to those reported previously [17], in the transparency region of KTP crystals for all types of phase matching and various input data. Here, n_j is the refractive index for one of the three interacting waves with wavelength λ_j in the phase matching direction. FOM(λ_1,λ_2) distributions were described in detail previously [17, 18]. Figures 5a–5c show the distributions with the maximum FOM(λ_1,λ_2) value (FOM$_d$) in the phase matching directions, and Figs 5d–5i show the FOM(λ_1,λ_2) (FOM$_T$) distributions in the TNCPM directions with input data for $dn_i(\lambda)/dT$ (3) from Ref. [6] (Figs 5d–5f) and (4) from Ref. [5] (Figs. 5g–5i). The grey areas in Figs 5g–5i correspond to phase matching for the conversion process but without TNCPM. It is well seen that, at $dn_i(\lambda)/dT$ from Ref. [5], TNCPM is only possible in a very narrow wavelength range. This is in perfect agreement with the results presented in Fig. 4 and Table 2. In the case of the data from Ref. [6], TNCPM is possible in a considerably broader wavelength range than in the case of the data from Ref. [5].

Clearly, one cause of the considerable difference in thermo-optic parameters is that it is incorrect to use experimental data obtained for different crystals. This refers to the temperature bandwidths corresponding to TNCPM. In Table 1, to such a regime their correspond $2\Delta T$ values above 100 °C. The variation of conversion efficiency with temperature [9, 12] demonstrates that it differs significantly from $\text{sinc}^2(d\Delta k/dT\cdot\Delta T\cdot L/2)$ (where $\Delta k = k_3 - k_2 - k_1$, $k_j = 2\pi n_j/\lambda_j$, and L is the crystal length), corresponding to temperature-critical phase matching. This leads to a considerable error in temperature bandwidth and is due to the following: In the general case, the relation for the wave vector mismatch has the form

$$\Delta kL = \sum_m \frac{1}{m!}\frac{d^m\Delta k}{dT^m}\Delta T^m L. \qquad (5)$$

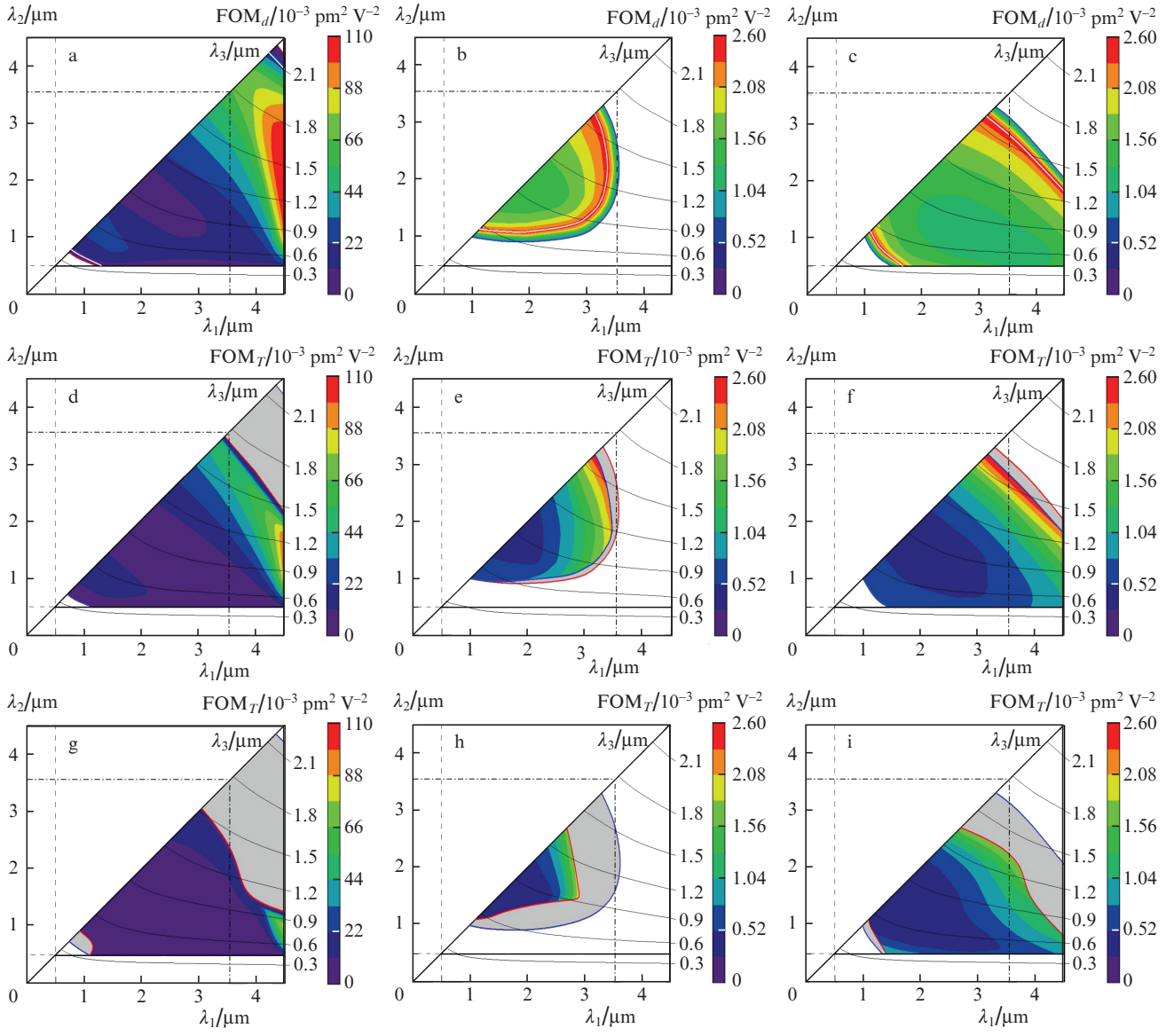

Figure 5. FOM distributions for ssf (a, d, g), sff (b, e, h), and fsf (c, f, i) phase matching with the maximum value FOM$_d$ (a–c) and FOM$_T$ in TNCPM directions (d–i) at various input data for $n_i(\lambda)$ (2) (a–i) and $dn_i(\lambda)/dT$ (3) (d–f) and (4) (g–i).

In the case of temperature-critical phase matching (at $d\Delta k/dT \neq 0$ and $d^m\Delta k/dT^m = 0$), $2\Delta T$ is a linear function of L. Because of this, the reference value $2\Delta T_{ref}$ (in °C cm) given for a 1.0-cm-long crystal is related to the experimentally measured $2\Delta T_{exp}$ for a crystal of arbitrary length L by $2\Delta T_{ref} = 2\Delta T_{exp} L_{exp}$.

In the case of mth-order temperature-noncritical phase matching (at $d\Delta k/dT = 0$ and $d^m\Delta k/dT^m \neq 0$), the relation has the form $2\Delta T_{ref} = 2\Delta T_{exp} L_{exp}^{1/m}$. In this case, $2\Delta T_{ref}$ has the dimensions of °C cm$^{1/m}$. If $d^m\Delta k/dT^m$ derivatives of various orders are comparable in magnitude, as in some studies, the relationship between L_{exp} and $L = 1.0$ cm is determined by the roots of the polynomial relation (5) at $\Delta kL/2 = 0.443\pi$. In this case, the dimensions of $2\Delta T_{ref}$ cannot be unambiguously determined.

For example, in the case of SHG at $\lambda = 0.9942$ μm in a 5-mm-long KTP crystal, Risk et al. [9] experimentally obtained a temperature bandwidth of 350 °C. They found that phase matching was temperature-critical with $2\Delta T_{ref} = 175$ °C cm [9]. This value is given in all publications and handbooks. The variation of conversion efficiency with temperature [9] points to TNCPM. The derivatives of various orders in (5) make comparable contributions. In the absence of data on the second and higher order derivatives for $dn_i(\lambda)/dT$, the temperature phase-matching bandwidth at $L = 1.0$ cm cannot be determined. In this case, the measured temperature bandwidth and crystal length ($2\Delta T_{exp}$ at L_{exp}) should be given. The temperature bandwidth $2\Delta T_{ref}$ calculated using data for the first derivative $dn_i(\lambda)/dT$ in the TNCPM regime cannot be compared to measured $2\Delta T_{exp}$. If there are incomplete $dn_i(\lambda)/dT$ data in the case of TNCPM, one can try to reach agreement not in terms of $2\Delta T$ but in terms of the phase matching directions in which this regime is possible.

The above results lead us to the following general conclusion: At present, manufacturers of KTP crystals use a number of crystal growth processes and their modifications. In most cases, high-temperature solution growth is employed, with various solvents and crystallisers. As a result, the difference in phase matching angles for various frequency conversion processes can reach 10° and more. In addition, one grows mixed crystals (Rb:KTP, Nb:KTP, Cs:KTP, and others). Particular growth processes are the know-how of manufacturers. Reported experimentally measured temperature phase-matching bandwidths were obtained for crystals grown by different processes. With such a difference in parameters, each process requires individual fitting equations for $n_i(\lambda)$ and $dn_i(\lambda)/dT$. One fails to find general and versatile relations for homogeneous and mixed crystals. For homogeneous media, the most accurate relations describing thermo-optic parameters ($dn_i(\lambda)/dT$) of KTP crystals, which allow one to calculate temperature phase-matching bandwidths and temperature-noncritical processes, were reported by Kato [6] [relations (3)], in combination with data for $n_i(\lambda)$ refractive indices from Ref. [5] [relations (2)].

In conclusion, it should be noted that Gagarskiy et al. [17] reported results of research on functional capabilities of KTP and isomorphous (RTA, RTP, KTA, and CTA) crystals in their transparency regions for all frequency conversion applications. They presented results for the maximum effective nonlinearity coefficient in phase matching directions and TNCPM directions. For KTP crystals, $dn_i(\lambda)/dT$ data from Ref. [6] were used. Whereas conversion processes with TNCPM in KTP crystals are possible in a wide wavelength range, in the case of KTA such a range is considerably narrower. In CTA crystals, TNCPM is impossible. The results presented in Fig. 5 suggest that it is necessary to revise $dn_i(\lambda)/dT$ data for all crystals of the above group.

References

1. Zumsteg F.C., Bierlein J.D., Gier T.E. *J. Appl. Phys*., **47**, 4980 (1976).
2. Nikogosyan D.N. *Nonlinear Optical Crystals: A Complete Survey* (Springer-Verlag, 2005).
3. Chen Q., Risk W.P. *Electron. Lett*., **30**, 1516 (1994).
4. Kato K. *IEEE J. Quantum Electron*., **27**, 1137 (1991).
5. Kato K., Takaoka E. *Appl. Opt*., **41**, 5040 (2002).
6. Kato K. *IEEE J. Quantum Electron*., **28**, 1974 (1992).
7. Garmash V.M., Ermakov G.A., Pavlova N.I., Tarasov A.V. *Sov. Tech. Phys. Lett*., **12**, 505 (1968) [*Pis'ma Zh. Tekh. Fiz.*, **12**, 1222 (1986)].
8. Garmash V.M. Personal communication (2005).
9. Risk W.P., Payne R.N., Lenth W., Harder C., Meier H. *Appl. Phys. Lett*., **55**, 1179 (1989).
10. Fan T.Y., Huang C.E., Hu B.Q., Eckardt R.C., Fan Y.X., Byer R.L., Feigelson R.S. *Appl. Opt*., **26**, 2390 (1987).
11. Kishimoto T., Imamura K., Ito M. *Proc. Autumn Meet. Japan Soc. Appl. Phys. (JSAP)* (Tokyo, 1991).
12. Grechin S.G., Dmitriev V.G., D'yakov V.A., Pryalkin V.I. *Quantum Electron*., **28**, 937 (1998) [*Kvantovaya Elektron*., **25**, 963 (1998)].
13. Shen H.Y., Zhou Y.P., Lin W.X., Zeng Z.D., Zeng R.R., Yu G.F., Huang C.H., Jiang A.D., Jia S.Q., Shen D.Z. *IEEE J. Quantum Electron.*, **28**, 48 (1992).
14. Ou Z.Y., Pereira S.F., Polzik E.S., Kimble H.J. *Opt. Lett.*, **17**, 640 (1992).
15. Abrosimov S.A., Grechin S.G., Kochiev D.G., Maklakova N.Yu., Semenenko V.N. *Quantum Electron*., **31**, 643 (2001) [*Kvantovaya Elektron*., **31**, 643 (2001)].
16. Kato K. *IEEE J. Quantum Electron*., **27**, 1137 (1991).
17. Gagarskiy S., Grechin S., Druzhinin P., Kato K., Kochiev D., Nikolaev P., Umemura N. *Crystals*, **8**, 386 (2018).
18. Andreev Yu.M., Arapov Yu.D., Grechin S.G., Kasyanov I.V., Nikolaev P.P. *Quantum Electron*., **46**, 995 (2016) [*Kvantovaya Elektron*., **46**, 995 (2016)].